

BLAST EFFECTS ON AIR CLEANING EQUIPMENT - Results  
of Filter Tests

Charles E. Billings, Richard Dennis, and Leslie Silverman  
Harvard School of Public Health  
55 Shattuck Street  
Boston 15, Massachusetts

SUMMARY

This report summarizes results of studies of the effect of shock waves impressed on air filters in a direction opposite to normal air flow.

Moderate damage to Dust-Stop prefilters occurs at shock overpressures greater than one inch of mercury, severe damage occurring at pressures greater than three inches of mercury. At one inch over-pressure large amounts of dust are removed from the filter but physical damage is slight. Pleated A.B.C. No. 1 filters (24 x 24 x 6 inch) were found to sustain moderate damage at a pressure of six inches of mercury and a pressure of ten inches caused complete destruction. Pressures of five inches of mercury or less caused no apparent physical damage. A filter with perforated aluminum plates nailed to both faces had no additional strength to resist blast pressure.

Reentrainment studies have indicated large amounts of dust will be dislodged from a filter by the action of a shock wave.

---

This study was made under Contract No. AT(30-1)841 between the U. S. Atomic Energy Commission and Harvard University. Opinions expressed are those of the authors and do not necessarily represent the views of the U. S. Atomic Energy Commission.

At the request of the Division of Engineering, U.S. Atomic Energy Commission, Washington, D. C. an investigation into the effects of shock waves on air cleaning devices has been undertaken at the Harvard University Air Cleaning Laboratory. Major objectives of this study are:

1. To determine what structural damage occurs to air cleaning devices when they are subjected to a shock wave in a direction opposite to normal air flow;
2. To determine how much captured dust may be reentrained from the air cleaner and its connecting ductwork by the blast effect;
3. To develop inexpensive methods for reducing damage and minimizing reentrainment.

This report discusses expected damage to Dust-Stop roughing filters and A.E.C. No. 1 filters (and reentrainment of dust from A.E.C. No. 1 filters) at various blast over-pressure levels.

#### 1. Test Equipment

A 20 inch diameter shock tube has been constructed with a transition to and from a 24 x 24 inch square section to provide for location of test equipment as shown in Figure 1. The shock tube is attached to a 20 inch diameter air lock on an 8 foot diameter by 10 foot long compression chamber. A steel ring and clamp at the inner face of the lock hold layers of brown Kraft wrapping paper which burst at predetermined tank pressures. Rupture of this paper disc creates

a shock wave which is propagated down the tube to the test section. The wave is dissipated in a pressure relief chamber at the end of the tube (about 20 feet from the test area) by a double layer cinder block wall. The pressure is relieved through a perforated wall of the relief chamber. Over-pressures are recorded by a sensitive bellows placed in the wall of the tube just prior (6 inches) to the test section. A mirror mounted on the rear of the bellows deflects a light beam and the trace is recorded on photo-sensitive paper.

Before testing a filter, a number of layers of paper were ruptured to determine the magnitude of the wave produced. From this calibration, which varies somewhat due to weather conditions, a reliable estimate could be made of the strength of the shock wave to be impressed on the filter. With a filter in place the over-pressure is substantially increased at the test section as indicated by shock wave theory.

## 2. Test Results

### a. Blast Damage

Initial tests were made on damage to Dust-Stop pre-filters at various over-pressure levels. These are 20 x 20 x 2 inch Fiberglas mats held in a cardboard frame with light gage metal retaining screens on each face. The results of this series are presented in Table 1, tests 1 to 5. These filters will not withstand over-pressures greater than about one inch of mercury without sustaining some damage. Pressures near 3 inches of mercury caused complete failure

and the Fiberglas media was carried down the tube into the receiving chamber. It was observed that substantial dust was reentrained from the filter even though structural damage was slight at lower pressure levels.

Several 24 x 24 x 6 inch "absolute" type (A.E.C. No. 1) pleated space filters were tested for damage levels in the same manner (Table 2). Slight structural damage occurs when over-pressures reach about 6 inches of mercury. Complete failure occurs at pressures of 10 inches of mercury. Typical failure is shown in Figures 2 and 3. Three filters (tests 10, 11, and 12) were tested to determine air flow characteristics before and after blast, and also to check mechanical strength of perforated aluminum plates nailed to both faces (as supplied by manufacturer in some cases.) A standard 24 x 24 x 6 inch filter tested at 6.2 inches of mercury over-pressure showed moderatedamage. The pleats were pushed away from the blast about 1/4 inch over about one-half the face area. Air flow resistance (at rated 500 cubic feet per minute) fell from an initial value of 0.80 inches of water to 0.76 inches of water after testing. The same test conditions (test 11) applied to a filter with perforated aluminum plates on both faces showed about the same amount of damage. The filter media and the rear plate were pushed back about one inch over about one-third of the area as shown in Figure 4. Air flow resistance fell from 1.30 (initially) to 1.06 inches of water after test. A third filter tested at 4.3 inches of mercury (test 12) showed no physical damage but its resistance

was decreased from 0.88 to 0.80 inches of water by the test. It is concluded that moderate to severe damage will be sustained by 24 x 24 x 6 inch pleated "absolute" (A.E.C. No. 1) filters at blast over-pressures greater than 5 inches of mercury. Filters subjected to moderate over-pressures may suffer some damage but may be suitable in emergency disaster situations.

b. Dust Reentrainment

Additional tests have been made on 24 x 24 x 6 inch and 12 inch pleated "absolute" type (A.E.C. No. 1) filters to determine the amount of dust displaced by sub-damage level blast waves. This study is presented in detail in Table 3. The 6 inch filter held about one-half pound of dust (Calcium Carbonate) for an increase of one inch in resistance at rated air flow (500 cubic feet per minute). The 12 inch filter held about one pound of dust for a one inch resistance rise at rated flow (1000 cubic feet per minute). These values were found to check approximately with data presented by Mr. Walter Smith (of Arthur D. Little Inc.), at the Third Air Cleaning Seminar at Los Alamos. Filters were loaded to various degrees with a known amount of dust and subjected to over-pressures of 4 (for 6 inch) to 5 (for 12 inch) inches of mercury. With one exception (noted in Table 3, test 14) no physical damage was apparent from these tests.

It is concluded that at over-pressures just below damage levels (1) filters loaded to 100% capacity lose about 90% of this dust, and (2) filters loaded to 10% of capacity lose about 40% of this dust. The dust was carried down the shock tube and into the pressure relief chamber, and in fact,

was dispersed quite generally all over the testing area. High-volume air samples taken in the shock tube about 2 feet behind the test filter, and at the outlet of the tube into the relief chamber indicated air concentrations ranging from 18 to 20 grains per cubic foot for the 12 inch filter when fully loaded (tests 19 and 20) to no measurable amount when filters were loaded to 10% of capacity. A calculated value of air concentration based on pressure rise in the compression chamber before rupture of the diaphragm indicated air concentrations as high as 68 grains per cubic foot are possible. Large amounts of air-borne dust are produced by blast wave effects on loaded filters. The pressures (4 to 5 inches of mercury) used in this test series correspond to a distance of 6000 to 8000 feet from ground zero of a nominal atomic bomb. Blast wave duration time was of the same order of magnitude for this distance from ground zero, about 0.8 to 1 second.

#### c. Further Investigations

Further study is underway to determine the reentrainment from pleated filters at lower over-pressures. Damage levels for 24 x 24 x 12 inch filters will be determined. These studies have suggested some inexpensive methods for increasing damage levels for filters, and these will be investigated.

TABLE 1

## Shock Tube Tests of "Dust-Stop" Fiberglas Prefilters - Failure Pressure

Test No.	Number of Sheets in Diaphragm	Diaphragm Rupture Pressure "Hg	Remarks
1	4	6	Complete failure. Both screens and Fiberglas carried down tube to receiving chamber.
2	2	3	Complete failure. Both screens remained attached to the filter frame but the Fiberglas was carried down the tube about 12'.
3	1	1.5	Partial failure. Downstream screen bent away from blast slightly. Large quantity of fly ash reentrained and carried into pressure relief chamber.
4	3	4.5	Complete failure. Upstream (blast side) screen remained in place, downstream screen and Fiberglas carried down into receiving chamber.
5	3	6	Complete failure. No large pieces of Fiberglas remained impinged on cinder block wall and some penetrated through two layers. Most complete destruction.

TABLE 2

Shock Tube Tests of AEC "Absolute" Type (No. 1) Pleated Filters<sup>a</sup> - Failure Pressure

Test No.	Diaphragm Rupture Pressure at Filter "Hg"	Measured Pressure at Filter "Hg"	Pressure Characteristic No. Cycles	Trace Characteristics Time to Return to Zero	Filter Resistance <sup>b</sup> in. w.g.		Remarks
					Initial	Final	
5	5.0	8.3	1	0.80	-	-	No apparent damage.
6	10.0	>20.0	3	1.45	-	-	Complete failure (same filter as Test 5).
7	4.2	6.3	1	0.72	-	-	No apparent damage.
8	5.4	11.8	1	0.89	-	-	Partial failure over 1/3 of area. Pleats pushed back 1/4" (same filter as test 7).
9	5.0	12.4	2.5	1.22	-	-	Complete failure (same filter as Tests 7 and 8).
10	6.2	14.0	1	0.86	0.80	0.76	Partial failure, rear pushed back 1/4"
11	6.4	12.2	1	2.86	1.30	1.06	Partial failure, perforated aluminum plates nailed to each face. Rear plate pushed back by pleats about 1".
12	4.3	9.0	1	0.92	0.88	0.80	No apparent damage.
13	12.0	>20.0	1.5	0.86	-	-	Complete failure (same filter as Test 12).

a. 24" x 24" x 6" b. At 500 cfm



TABLE 3. Shock Tube Tests of ACC<sup>a</sup> Absolute<sup>b</sup> Type (No. 1) Pleated Filters - Reentrainment Study

Test No.	Filter Size <sup>a</sup>	Hg Diaphragm Rupture at Filter	Pressure Trace Characteristics		Filter Resistance <sup>b</sup>		Filter Load		Load Removed		Air Concentration, Grains/cu.ft.		Remarks
			Nb. Cycles	Time to Return to Zero, sec.	Clean	In. w.g. Loaded	Grains	%	Grains	%	From Filter	Outlet of Tube	
14A	-	5.3	5.7	1.49	-	0.90	1.69	-	-	-	-	-	Calibration
14B	6	3.4	-	-	-	-	206	100	114	55	1.2	1.8	Test, partial failure pleats moved back 1/8"
15A	-	3.6	4.5	1.53	-	-	-	-	-	-	-	-	Calibration
15B	6	3.6	-	-	-	-	-	-	-	-	-	-	Test to recheck 14B
16A	-	3.6	4.5	1.42	-	-	-	-	-	-	-	-	no apparent damage
16B	6	3.4	5.2	0.66	0.73	1.57	155	78	152	98	5.5	4.1	Calibration
17A	-	3.6	5.2	1.47	-	-	-	-	-	-	-	-	Test, no damage
17B	6	3.7	5.8	0.72	0.77	1.15	126	56	74	59	3.4	1.4	Calibration
18A	-	3.5	3.8	1.23	-	-	-	-	-	-	-	-	Test
18B	6	3.8	9.5	0.95	0.84	0.92	26	10	8	32	0	0	Calibration
19A	-	4.6	6.9	1.47	-	-	-	-	-	-	-	-	Test
19B	12	5.0	8.8	0.79	0.97	1.92	429	100	359	84	17	9.9	Calibration
20A	-	5.3	6.0	1.29	-	-	-	-	-	-	-	-	Test
20B	12	5.1	7.4	0.71	0.99	1.91	417	100	396	95	20	7.2	Calibration
21A	-	4.5	5.9	1.52	-	-	-	-	-	-	-	-	Test
21B	12	4.7	9.4	0.76	1.04	1.12	39	8	20	51	0	0	Calibration
													Test

<sup>a</sup>2 1/2" x 2 1/2" x depth shown<sup>b</sup>At rated volume of 500 cfm for 6" and 1000 cfm for 12"

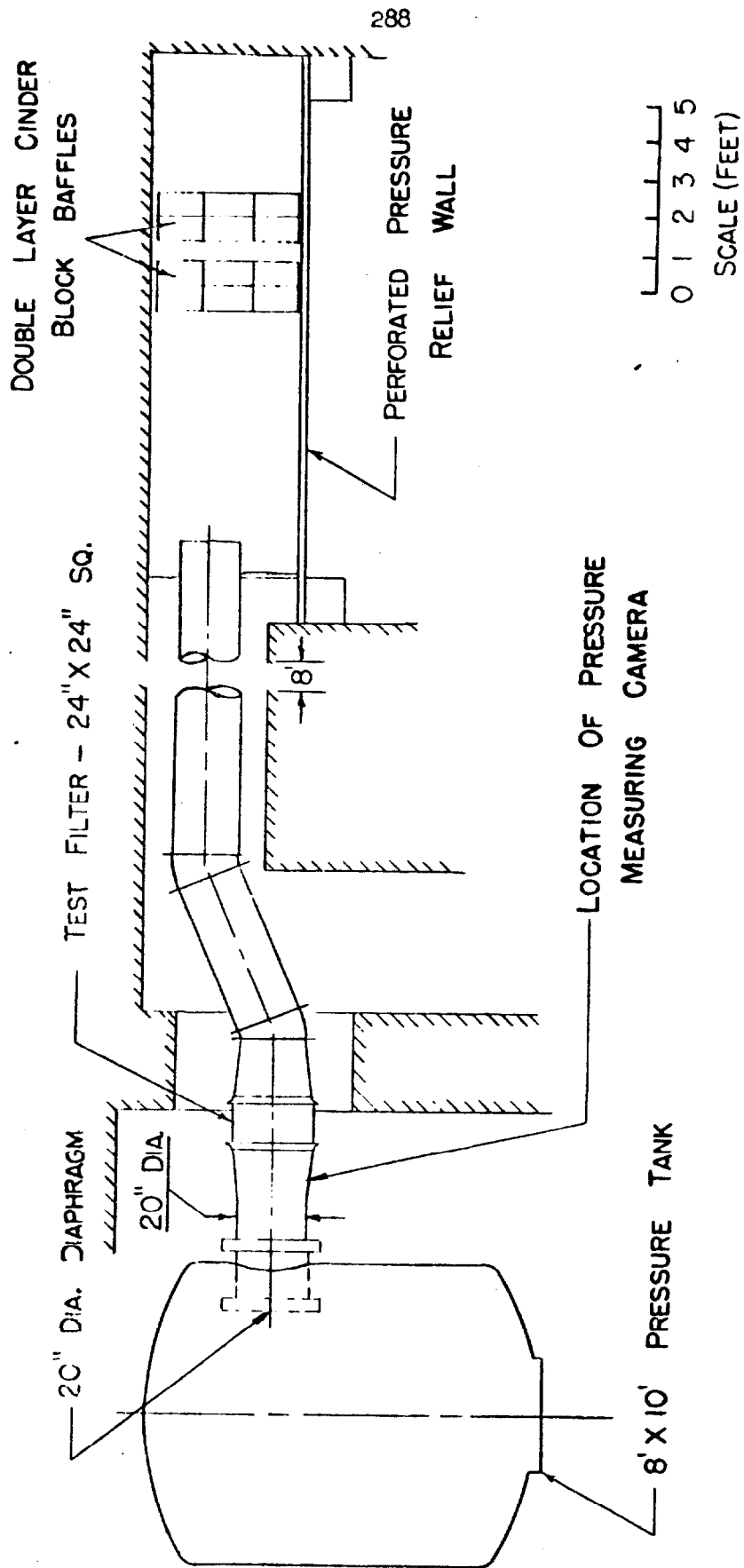


Figure 1. Experimental Shock Tube - Plan View

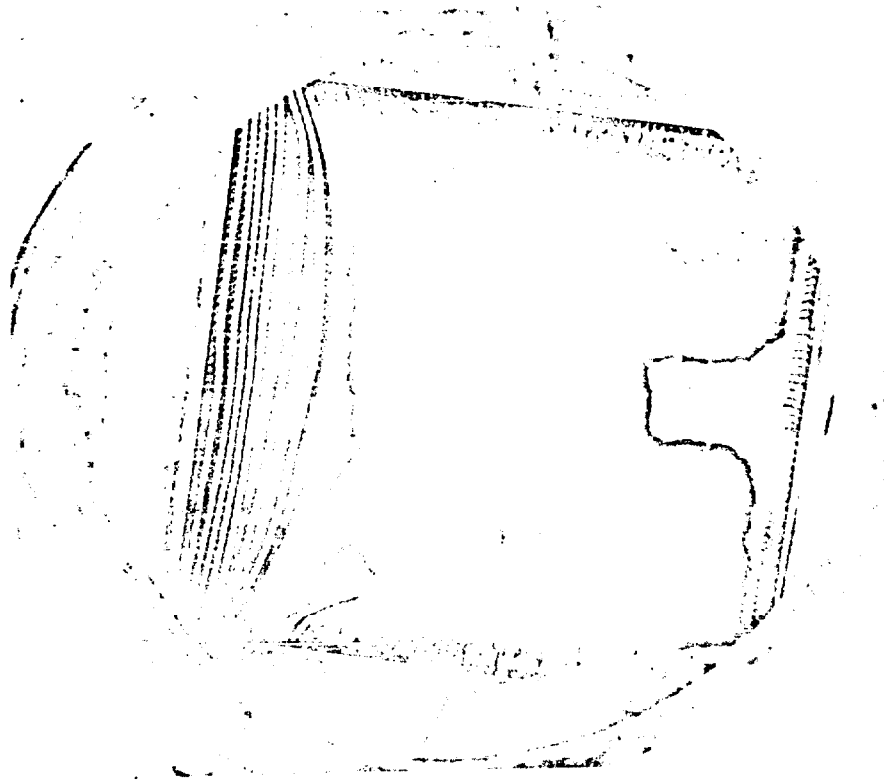


Figure 2. Pleated Paper Filter Showing Failure-  
Frame In Test Location In Shock Tube

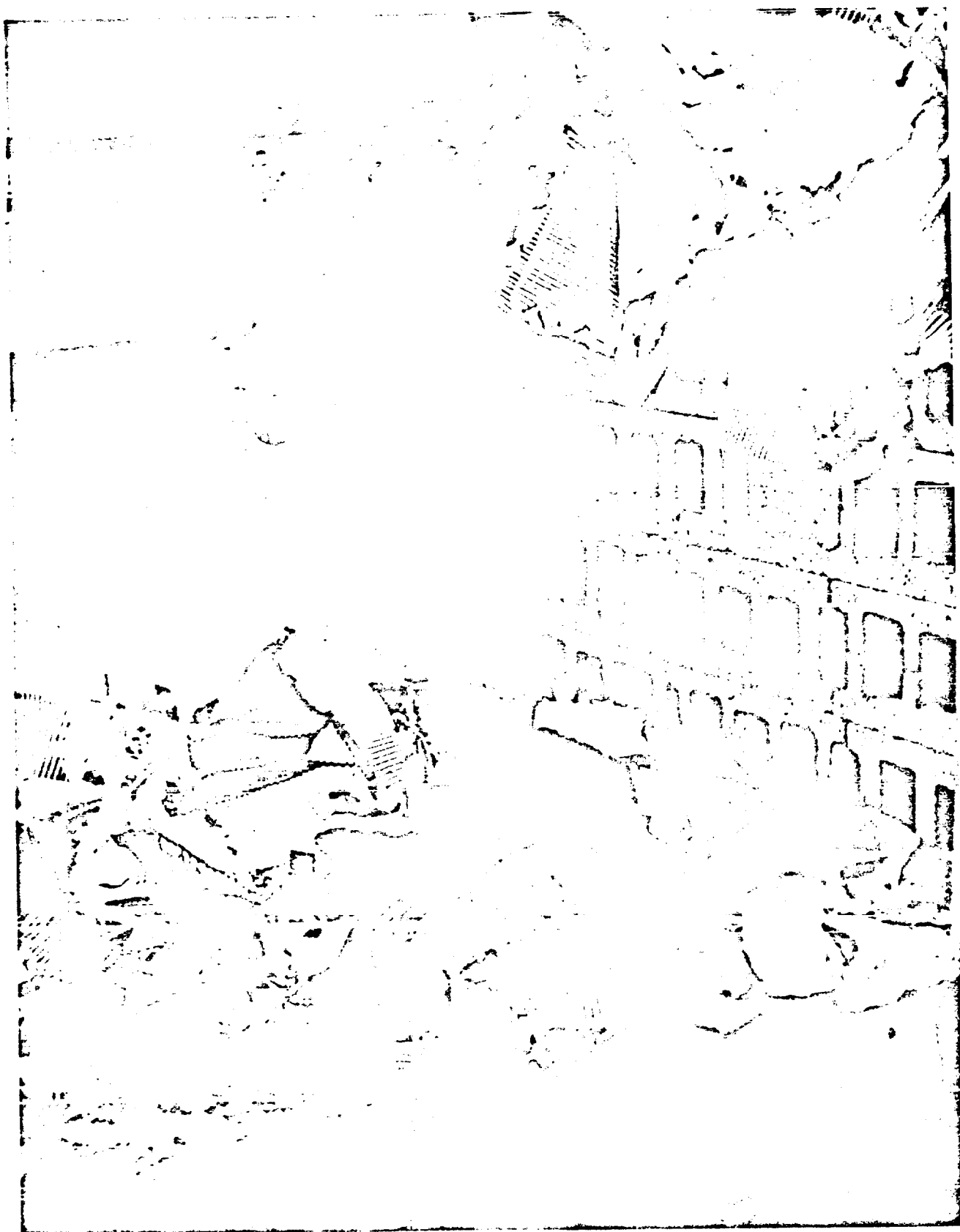


Figure 3. Pleated Paper Filter Showing Failure- Receiving Area

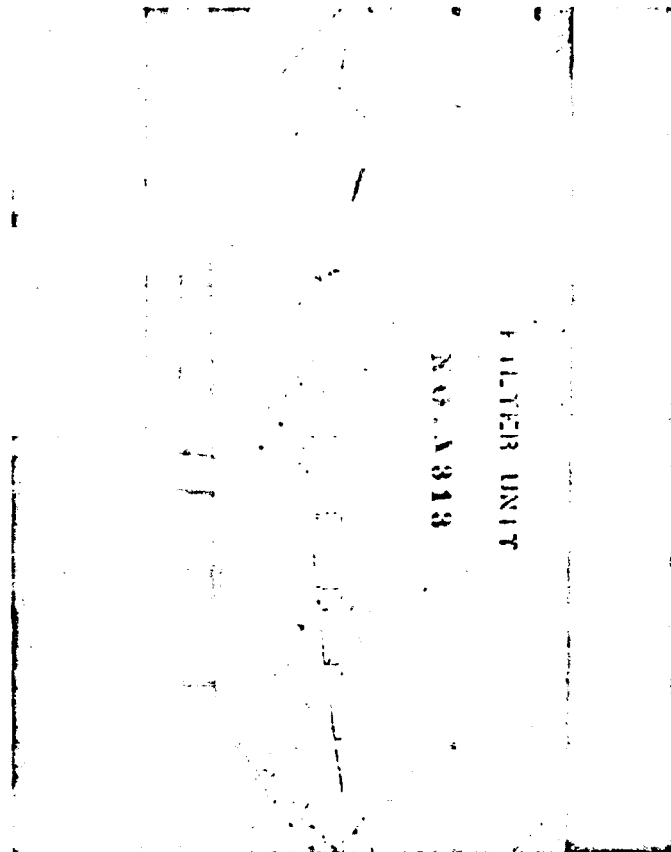


Figure 4. Pleated Paper Filter With Aluminum  
Plates- Partial Failure

## PROPERTIES OF AEROSOL AGGLOMERATES

W. J. Scheffy

The process of coagulation in aerosols of both liquid and solid particles has been widely studied. The effects of various factors on the rate of coagulation have been investigated. Less work has been done on the nature of the agglomerated particles formed in the process. Coalescence of drops presents no problem in this respect. But the properties of solid agglomerates differ greatly from those of the pure solid particles and, furthermore, vary widely with agglomerate size, circumstances of formation and other factors. The density and drag diameter are particularly important in many methods of air sampling or cleaning. Measurements with a jet impactor, for instance, yield a quantity which can be converted into a size distribution only if the density of the particles is known. This quantity is the impaction parameter

$$\Psi = CD^2 \rho v_0 / 18 \mu D_c$$

a dimensionless measure of the ratio of the particle inertia to the resistant force of the fluid on the particle (7). It has been shown that collection efficiency for various impactors and conditions, within certain limits, has a unique relationship to  $\Psi$ , so that substitution of the known quantities into the expression for  $\Psi$  gives a characteristic particle diameter for one impactor stage. With a cascade impactor the size distribution of an aerosol may be obtained. If  $\rho$  is unknown, all that is obtained is a distribution of the quantity  $CD^2 \rho$ , which, incidentally, is directly proportional to the free fall terminal velocity. This quantity is enough for some purposes, but not for an idea of the actual size of the airborne particles.

The fact that the density of solid agglomerates varies extremely from the normal solid density is to be expected, and early work with smoke particles proves it. Whytlaw-Gray and Patterson found particle densities lower than ten per cent of the normal solid value (9). In the present work the method used by these observers and others (1) has been extended to the measurement of drag diameters and densities for agglomerates of a number of substances. The experiments are simply an adaptation of Millikan's oil-drop measurements of the electronic charge (6). The velocities of a particle in free fall and rising under an electrical force are measured by observation with a low-power microscope, using a dark field and an eyepiece scale. Such data for one particle are sufficient to calculate two of the three variables involved: particle drag diameter, particle mass, and the value of the electronic charge. In the original experiments with oil drops the density of the particle was that of the pure liquid, so the particle size and the electronic charge could be obtained. Since the value of the electronic charge is now fairly well established, it can be used to determine both the other variables when they are unknown, as in the case of agglomerates.

The Millikan cell used was a standard model built for the Central Scientific Company. The plate spacing was three millimeters, with battery voltages ranging from 90 to 270, depending on the average particle mass of the aerosol used. By a number of precautions, such as filtering the light from the source and keeping the room temperature constant, convection and photophoretic effects were reduced to very low levels even without a constant-temperature bath surrounding

the cell. The particles were introduced into the cell by spraying from an aspirator or from a glass nebulizer which, although made for solutions or liquid suspensions, was found quite useful for dry powders. For one particle the free fall velocity and from five to ten different velocities of rise under the electric field were measured, the different electrical velocities corresponding to different particle charges. The calculations require these velocities for various charges because, although the magnitude of one electronic charge is known, it cannot be said a priori how many unit charges the particle has. The numbers of electrons corresponding to the various observed velocities can only be deduced by comparison of the velocities; the smallest observed difference between two velocities then corresponds to a difference of one electronic charge, if enough measurements have been made.

The equations involved are simple force balances. Both in free fall and in rise under the electric field a terminal velocity is reached in a matter of microseconds; the sum of the forces acting on the particle is then zero. In the first case,

$$mg = 3\pi\eta Dv_g/C \quad (1)$$

If the particle is rising in the electric field,

$$neX - mg = 3\pi\eta Dv_e/C \quad (2)$$

The two unknowns  $D$  and  $m$  can be obtained from these two independent equations. It should be noted that the  $D$  calculated here is actually the drag diameter, defined by Hawksley (4) as the value of  $D$  which satisfies the Stokes law of resistance. It is perhaps also noteworthy that the mass of the particle can be obtained without assuming anything



about the resistant force except that it is proportional to the velocity and has the same form with or without the electrical force acting. For, by dividing (1) by (2) and rearranging, we obtain

$$m = neXv_g/g(v_e+v_g)$$

All the coefficients of  $v_g$  and  $v_e$  cancel in the division. The calculation of  $D$ , of course, requires the explicit form of Stokes' law, and much of the scatter in the data is attributable to this approximation. When  $D$  and  $m$  are known, an approximate density can be calculated.

As a check of the method and apparatus, uniform Dow polystyrene spheres were measured. The diameter of the spheres was known very accurately from electron microscope observations by the manufacturer. The standard deviations for 0.514 and 1.171 micron spheres were 0.011 and 0.013 micron, respectively. The average error in the density of these spheres determined by the method above was less than five per cent. The deviations are probably due to convection, the difficulties of observation introduced by Brownian motion, and the uncertainty of the values of the Cunningham slip correction to Stokes' law. Several choices are possible for the Cunningham correction; those used here were based on experiments (2, 5, 8) with particles including sizes of the same order of magnitude as the mean free path of the gas molecules, the range of interest in this work.

Dispersal of more concentrated suspensions of the polystyrene produced agglomerates containing from two to thirty single spheres for the 0.514 micron particles, and up to 500 for another latex of 0.132

diameter spheres. Photomicrographs revealed two types of aggregate: spheroidal clumps and chains of moderate length. For agglomerates of uniformly sized particles of known mass, the number of particles per agglomerate can be easily ascertained by dividing the two masses. In this way four of the 0.514 micron agglomerates were shown to be doublets, and five of them triplets. The doublets all had drag diameters between 0.67 and 0.73 micron, the triplets between 0.80 and 0.84 micron. The exact significance of these values might be found by calculations similar to that of Faxen (3), who obtained a theoretical Stokes diameter for symmetrical doublets falling with their line of centers in a vertical position.

Table 1 shows all the substances measured, with their normal solid densities and the range of apparent densities of the agglomerates, calculated from the experimentally determined drag diameter and mass. Only for the polystyrene and the aluminum oxide were the primary particles homogeneous in size. The results have been plotted on log paper in the form  $CD^2_p$  versus mass (Figures 1 to 5). The equation of the lines is\*

$$CD^2_p = m^B$$

---

\*Note added January 18, 1956

The discovery of an error in the calculations indicates that this equation should read

$$CD^2_p = Am^B,$$

where A varies from about 1.1 to 2.2 for the substances used. Also, B varies so widely among these substances and others subsequently measured that the use of an average value is no longer justified. The range of variation of B is approximately 0.3 to 0.67. Figures 1 to 10 are still useful for showing the directions and orders of magnitude of the differences in behavior.

The solid line on each graph is the best line through the data for that substance. The dashed line represents the equation when the average value of B (0.644) for all the substances is used. The average deviation of the experimentally determined mass from this line is 32 per cent. The degree to which all the materials fit the same line is a measure of the similarity of both the densities and shapes of their agglomerates. In other words, it is a measure of the constancy of the relationship between mass and drag diameter for various real particles.

Figures 6 to 9 show the data obtained by previous observers (1,9) calculated in the same manner. The average equation

$$CD^2_p = m^{0.644}$$

thus may be said to hold, within the deviation noted, for materials with a range of normal density from 1.05 to 19.3 g./cc. and a range of primary particle size from 0.02 to 0.5 micron, dispersed in the manner of these experiments.

The behavior of particularly abnormal agglomerates is indicated by the curve for camphor smoke particles, which are well known to have a very open branched-chain structure (Figure 10). The data here fall 90 per cent below the average line; it may be significant that the slope is not greatly different. A tendency toward this type of behavior should be shown by agglomerates formed in the presence of excess electric charges, which promote chain formation.

As has been noted, the wide scatter of the data may be attributed to the wide variations in the overall shape of the agglomerates even of one substance. The smaller constant deviations shown by each material, however, are probably due to real differences

in the packing of primary particles in an agglomerate. There is no obvious correlation between these uniform deviations and any common properties of the substances, such as density, primary particle size, crystal habit, etc. The effect is of course a composite of more than one such factor. Further experiments are being carried out to shed light on the problem, particularly on the relationship of crystal form and surface structure to the packing.

Referring to the first problem discussed, size distributions of airborne agglomerates, the graph of  $CD^2_p$  versus mass may be used with the jet impactor to obtain drag diameter distributions for such aerosols. From the  $CD^2_p$  distribution measured by the impactor the distribution of particle masses can be obtained simply by reference to the curve. Allowance may be made for any available information on the general shape of the particles. Then  $m$  can be substituted into

$$CD^2_p = 6mC/\pi D = 6m(1 + 2A \lambda/D)/\pi D$$

to obtain  $D$ . A limitation is that the primary particles must not be so inhomogeneous that agglomerates widely different in size can have the same mass.

#### Acknowledgement

Most of the experiments and calculations in this work were performed by H. Herzig.

#### Literature Cited

1. Bar, R., Ann. Phys. 67, 157 (1922)
2. Ehrenhaft, J., and Wasser, E., Z. Phys. 37, 820 (1926)
3. Faxen, H., Z. Angew. Math. Mech. 7, 79 (1927)
4. Hawksley, P. G. W., Bull. Brit. Coal Util. Res. Assoc. 15, 105 (1951)

5. Hettlauch, J., Z. Phys. 32, 439(1925)
6. Millikan, R. A., Phys. Rev. 2, 109(1913)
7. Ranz, W. E., and Wong, J. B., Ind. Eng. Chem. 44, 1371(1952)
8. Reiss, H., Z. Phys. 39, 623 (1926)
9. Whytlaw-Gray, R., and Patterson, H. S., Proc. Roy. Soc. (London) 113A, 302(1926)

### Nomenclature

- A Factor in Cunningham correction, dimensionless
- B Exponent in empirical equation, dimensionless
- C  $= 1 + \frac{2A\lambda}{D}$ , Cunningham slip correction, dimensionless
- D Drag diameter of particle, cm.
- D<sub>c</sub> Characteristic dimension of collector in jet impactor, cm.
- e Electronic charge, electrostatic units
- g Acceleration of gravity, cm./sec.<sup>2</sup>
- m Mass of particle, gm.
- n Number of charge units on particle
- v<sub>0</sub> Velocity of air flow in jet impactor, cm./sec.
- v<sub>e</sub> Terminal velocity of particle under electrical force, cm./sec.
- v<sub>g</sub> Terminal velocity of particle in free fall, cm./sec.
- X Electric field strength, electrostatic units/cm.
- $\lambda$  Mean free path of air molecules, cm.
- $\mu$  Viscosity of air, gm./cm. sec.
- $\pi$  3.1416
- $\rho$  Density of particle, gm./cc.
- $\Psi = \frac{CD^2\rho v_0}{18\mu D_c}$ , impaction parameter, dimensionless

Table 1

Substance	Normal Density, g./cc.	Primary Particle Size, microns	Apparent Density of Agglomerates, g./cc.
Polystyrene	1.05	0.132	0.26-0.76
Polystyrene	1.05	0.514	0.15-0.97
Aluminum	2.70	less than 1	0.14-1.94
Aluminum oxide	3.99	0.02	0.14-1.45
Zinc oxide	5.61	0.05-0.1	0.86-2.50
Zinc	7.14	less than 1	0.57-3.27
Carbon (camphor smoke)	2.25		0.0091-0.0480

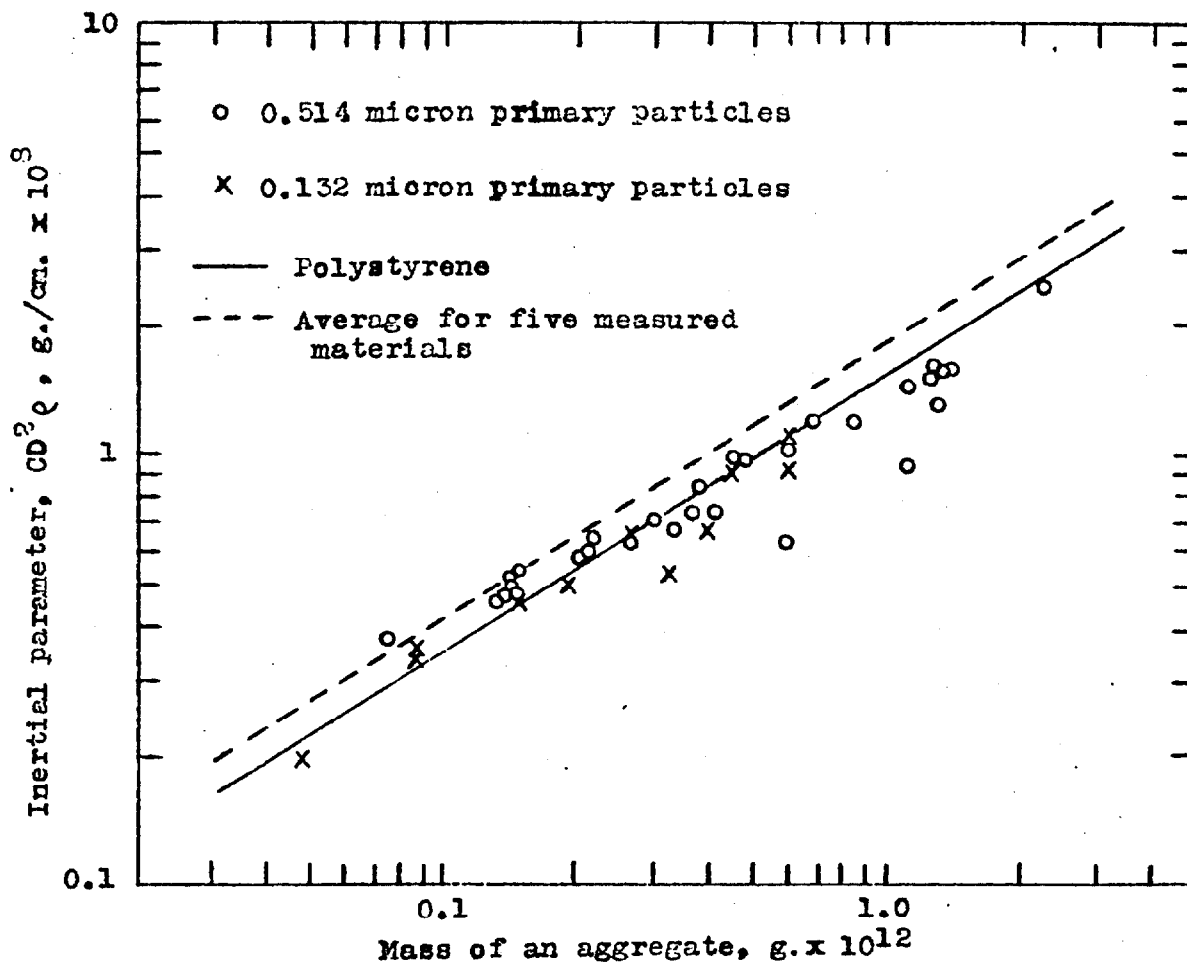


Figure 1. Relationship between mass and inertial parameter for polystyrene aggregates

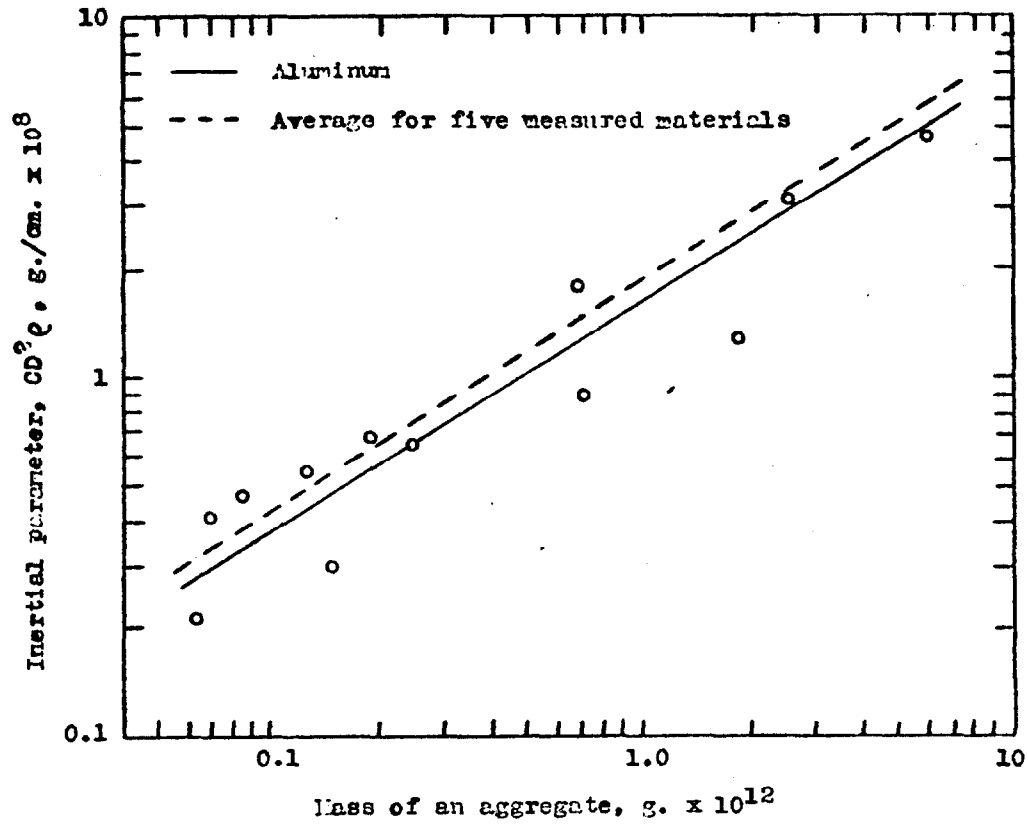


Figure 2. Relationship between mass and inertial parameter for aluminum aggregates

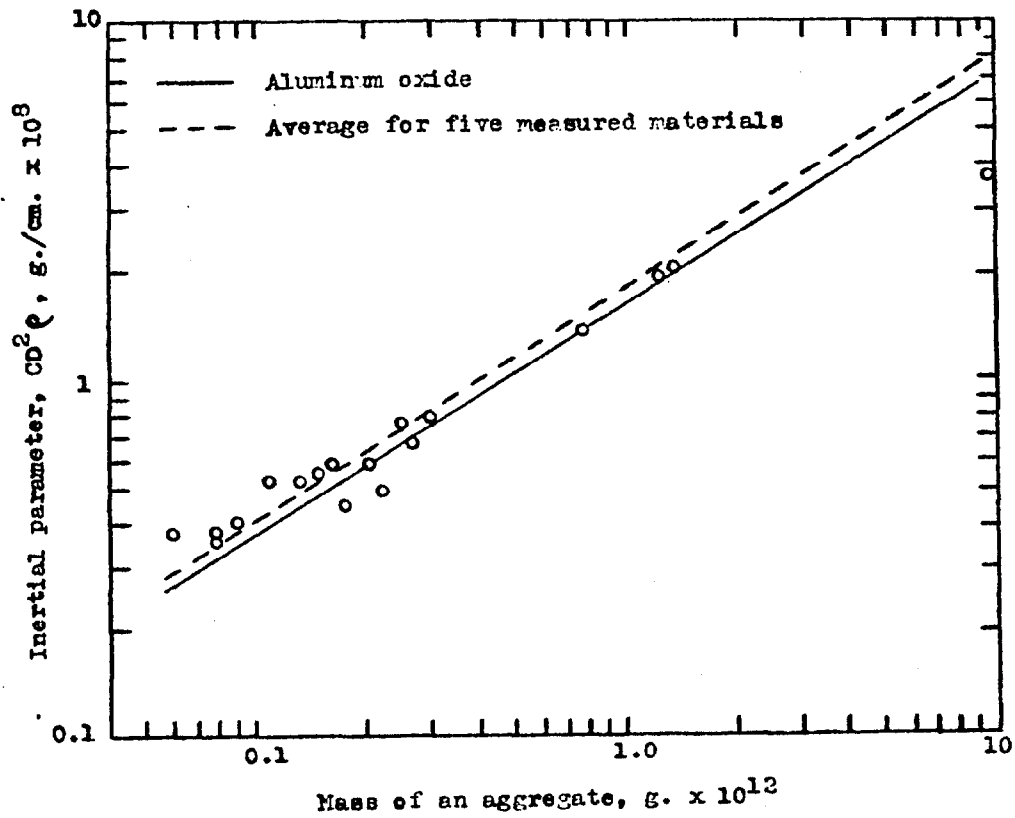


Figure 3. Relationship between mass and inertial parameter for aluminum oxide aggregates

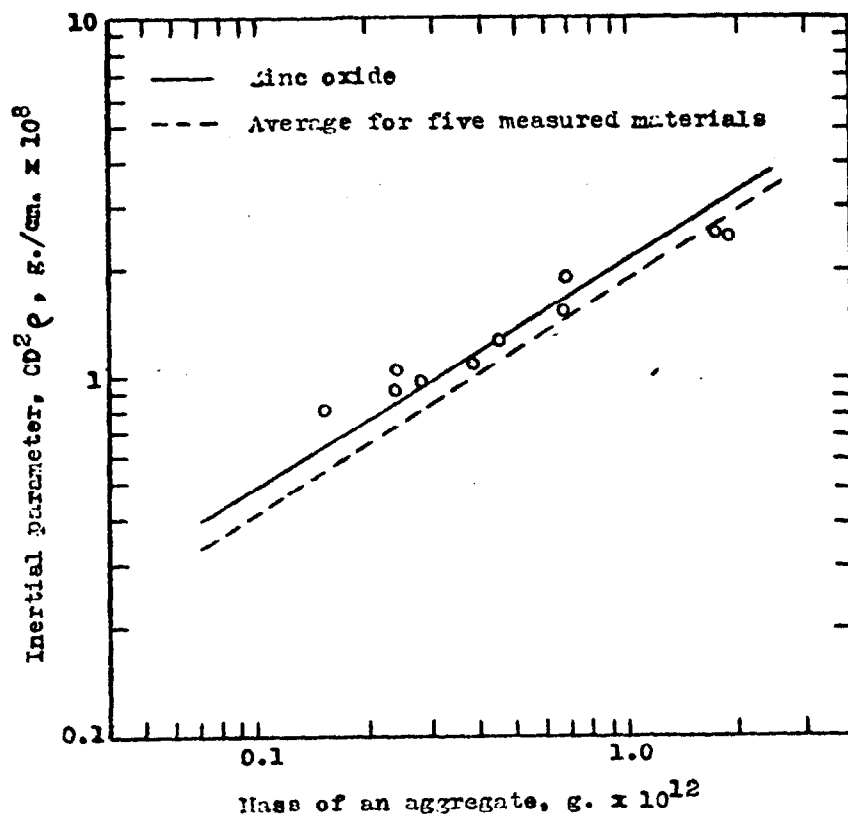


Figure 4. Relationship between mass and inertial parameter for zinc oxide aggregates

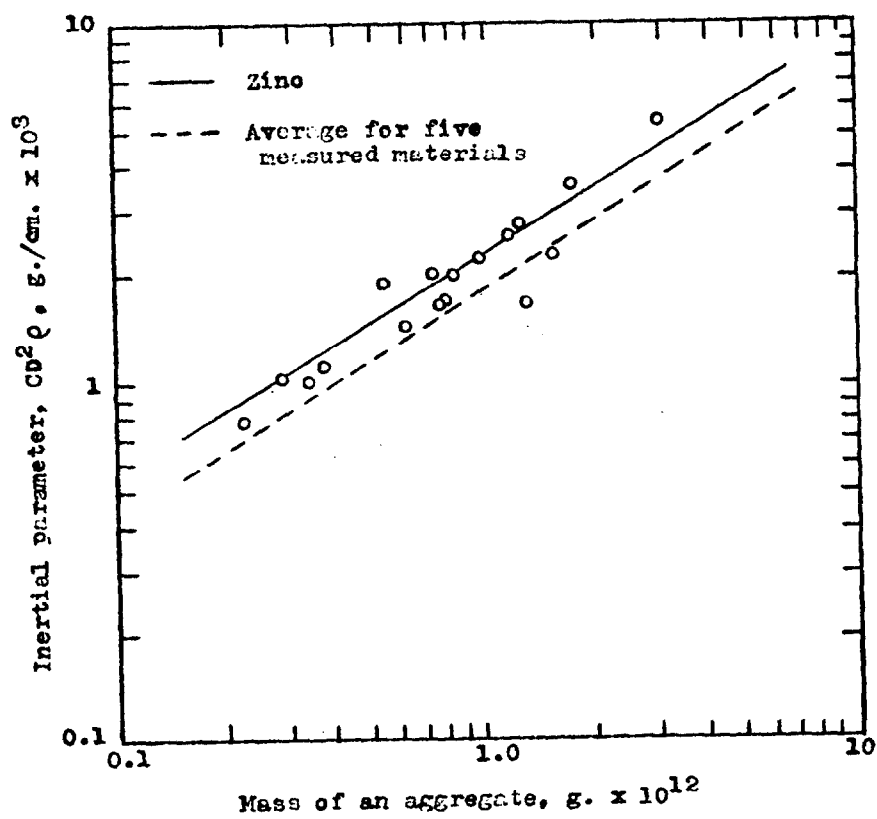


Figure 5. Relationship between mass and inertial parameter for zinc aggregates



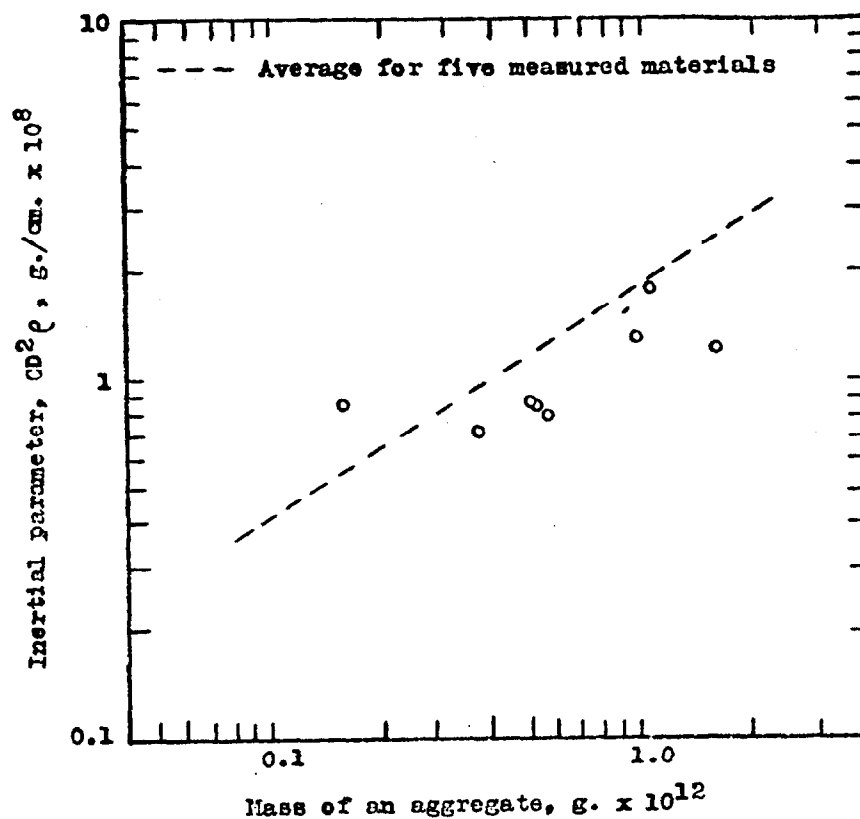


Figure 6. Relationship between mass and inertial parameter for cadmium oxide aggregates (18)

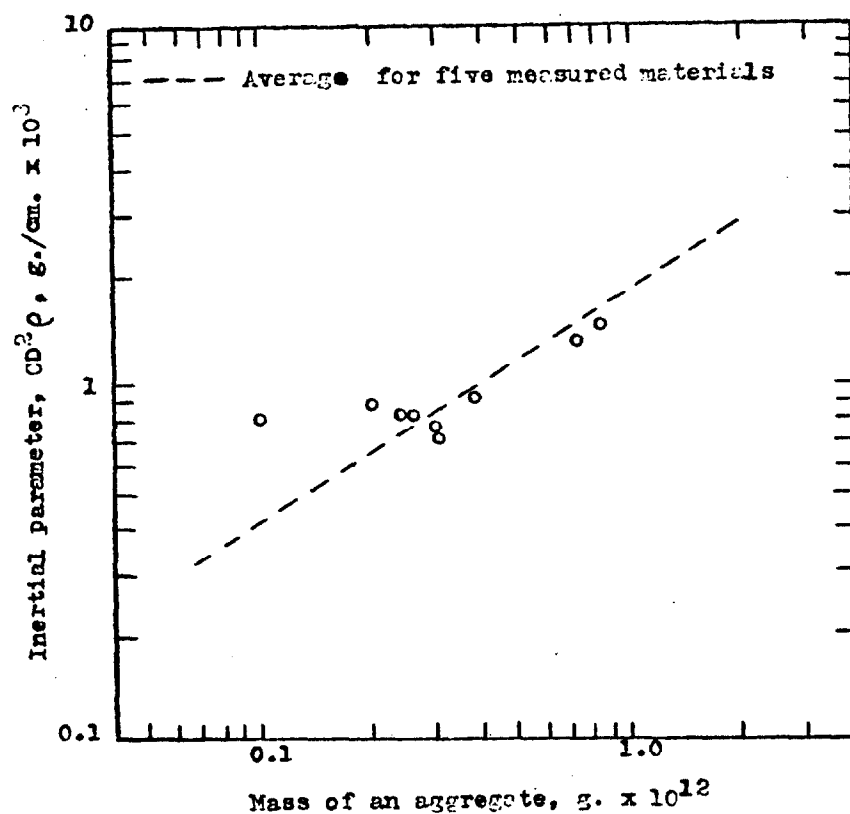


Figure 7. Relationship between mass and inertial parameter for silver aggregates (18)

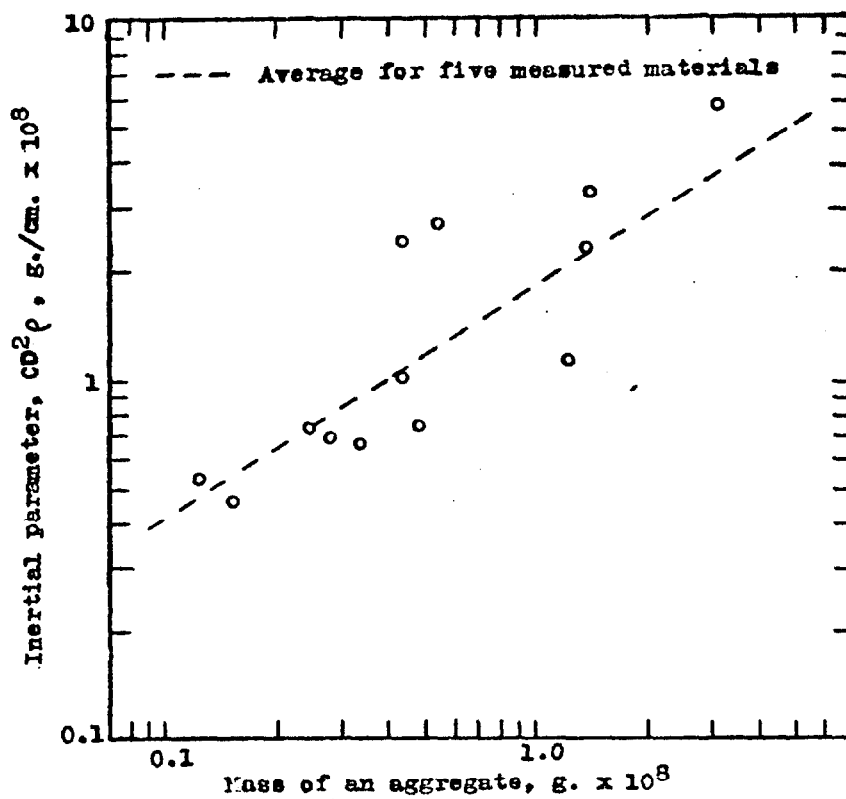


Figure 8. Relationship between mass and inertial parameter for gold aggregates (18)

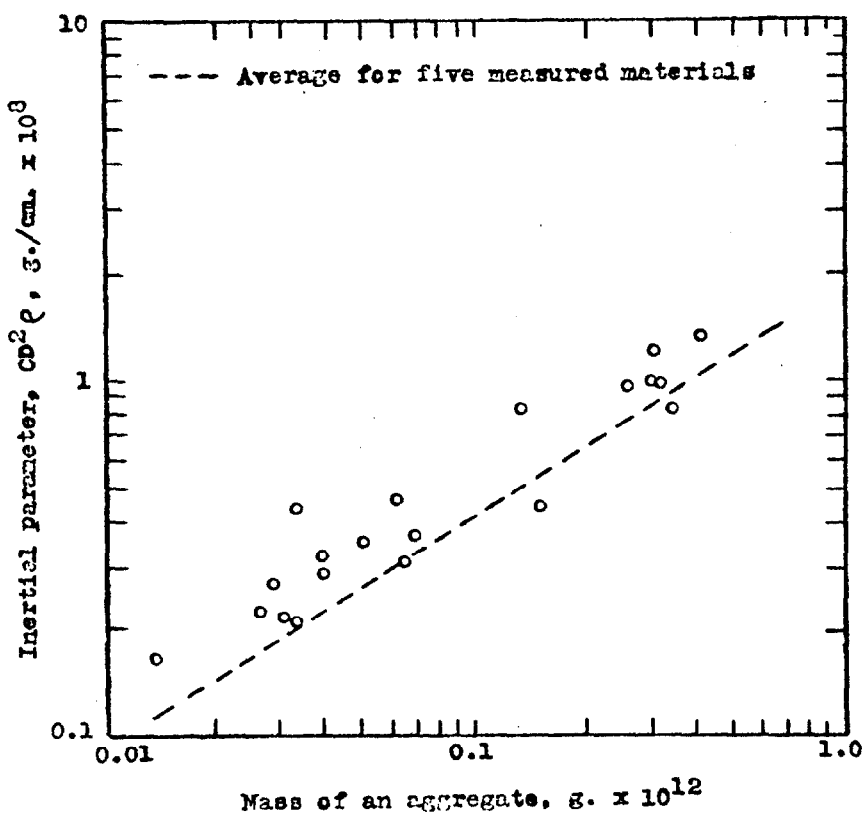


Figure 9. Relationship between mass and inertial parameter for selenium aggregates (1)

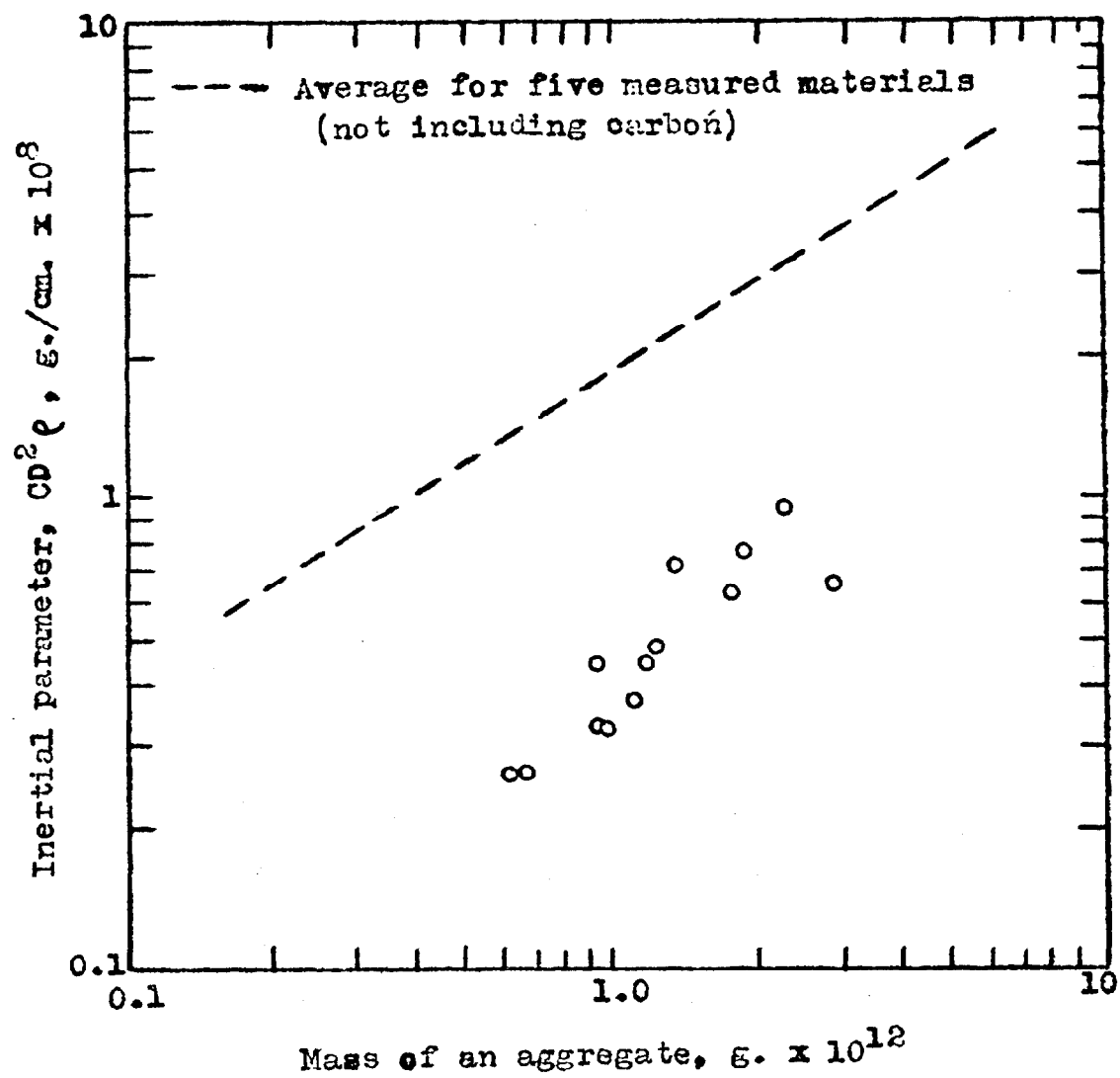


Figure 10. Relationship between mass and inertial parameter for carbon aggregates

# ABSORPTION OF NITROGEN OXIDES FROM WASTE GASES

By Max S. Peters

Engineering Experiment Station  
University of Illinois  
Urbana, Illinois

## Introduction

Many industrial processes evolve gases containing nitrogen oxides, and it is often necessary to effect removal or recovery of these oxides. In some cases, the gases must be cleaned before they can be released to the atmosphere, while, in other cases, efficient recovery of the nitrogen oxides is a direct and essential part of the manufacturing process.

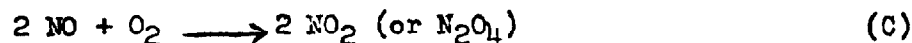
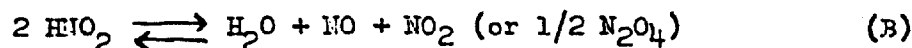
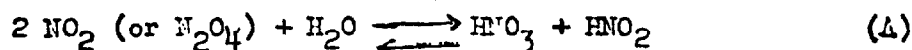
The removal of nitrogen oxides from gases becomes particularly difficult at low concentrations because the efficiency of most removal equipment decreases with reduction in oxide concentration. It is necessary, therefore, to understand the controlling mechanisms in the process before attempting to develop improved methods for removing nitrogen oxides from dilute gases.

The purpose of this paper is to present an analysis of the basic principles governing the absorption process and to show the results obtained when various types of equipment are used for removing nitrogen oxides from waste gases.

## Controlling Mechanism

Nitrogen oxides are commonly removed from gases by aqueous absorption accompanied by chemical reaction. The important nitrogen oxides in processes involving reactions with aqueous solutions are  $\text{NO}_2$ ,  $\text{N}_2\text{O}_4$ , and  $\text{NO}$ . Small amounts of  $\text{N}_2\text{O}_3$  and  $\text{N}_2\text{O}_5$  are also present in the gases, but these compounds rapidly come to equilibrium with  $\text{NO}$  and  $\text{NO}_2$  and represent only a small fraction of the total oxides at room or higher temperatures (6, 7).

The essential chemical reactions occurring in the removal process are:



Reaction (D) attains equilibrium rapidly and the equilibrium constant for this reaction is known as a function of temperature between 0°C and 90°C (8). The oxidation of NO proceeds relatively slowly although the reaction goes essentially to completion.

Reactions (A) and (B) are reversible and proceed at a finite rate. It is possible, therefore, that the rate of aqueous absorption is controlled by the rate of the chemical reactions. Diffusional resistance or a combination of diffusional resistance and chemical reaction rate could also control the rate of the aqueous absorption. The following integrated rate equations have been obtained for the two limiting cases of chemical reaction rate controlling (5) and gaseous diffusion controlling (4): (See table of nomenclature for notation)

Chemical reaction rate controlling,

$$\frac{1}{(p_{f\text{N}_2\text{O}_4})^{1/2}} = \frac{1}{(p_{o\text{N}_2\text{O}_4})^{1/2}} - 2\sqrt{K_p} \ln \frac{p_{o\text{N}_2\text{O}_4}}{p_{f\text{N}_2\text{O}_4}} + Bt \quad (1)$$

Gaseous diffusion controlling,

$$(p_{o\text{N}_2\text{O}_4})^{1/2} \left[ \frac{0.715}{\sqrt{K_p}} + (p_{o\text{N}_2\text{O}_4})^{1/2} \right]^{1.86} = F (p_{f\text{N}_2\text{O}_4})^{1/2} \left[ \frac{0.715}{\sqrt{K_p}} + (p_{f\text{N}_2\text{O}_4})^{1/2} \right]^{1.86} \quad (2)$$

The following assumptions were made in deriving Eqs. (1) and (2):

1. Chemical reactions occur under irreversible conditions.
2. Constant temperature and constant gas rate prevail.
3. Instantaneous equilibrium exists between NO<sub>2</sub> and N<sub>2</sub>O<sub>4</sub>.
4. Contact time is sufficiently short so that there is no appreciable oxidation of NO.

The theoretical and experimental results can be interpreted on the basis of plate efficiency. With this approach, the practical significance of the results is immediately apparent. Plate efficiency is defined as the amount of nitrogen oxides removed from the gases divided by the amount of oxides which would have been removed if the plate were theoretically perfect.

By choosing one experimental point as a basis, Eqs. (1) and (2) can be used to predict theoretical curves of plate efficiency versus  $e\text{NO}_2$  (i.e.,  $\text{NO}_2 + 2 \text{N}_2\text{O}_4$ ) content of the entering gases for the two possibilities of chemical reaction rate controlling and diffusion controlling. These two theoretical curves are presented in Figure 1.

Experimental tests were conducted to determine the controlling factors in the aqueous absorption of nitrogen oxides. The experimental data were obtained with a bubble-cap plate column under conditions of constant temperature, constant gas rate, irreversible reactions, negligible oxidation of NO while the gas was in contact with the liquid, and essentially instantaneous equilibrium between  $\text{NO}_2$  and  $\text{N}_2\text{O}_4$ . A dense mist was observed in the gas phase in all the runs.

The experimental results are presented in Figure 1 for comparison with the theoretical curves. As shown in Figure 1, the experimental plate efficiencies decrease with reduction in gaseous  $e\text{NO}_2$  concentration and follow the theoretical curve predicted for the case in which the controlling mechanism is the rate of the chemical reactions. In general, if operating equipment or operating conditions can be obtained which tend to eliminate chemical reaction rates as the controlling factor, the upper limit on the plate efficiency would be represented by the diffusion-controlling curve in Figure 1.

#### Effects of Operating Variables

Figure 2 shows the effect of temperature on the efficiency of nitrogen oxides removal from gases. As the operating temperature is increased, the removal efficiency decreases. If the rate of the chemical reactions controls the rate of the nitrogen oxides removal, the reduction in efficiency with increase in temperature can be attributed partly to the decrease in the fraction of  $e\text{NO}_2$  present as  $\text{N}_2\text{O}_4$ . On the same basis, an increase in operating pressure should give improved removal efficiencies.

The material used as the absorbing medium may affect the removal efficiency. Experimental results are presented in Figure 2 comparing the removal efficiencies for the cases in which water (or dilute nitric acid) and 20 per cent by weight aqueous sodium hydroxide were used as the absorbing media. As indicated in Figure 2, the removal efficiencies with aqueous sodium hydroxide as the absorbing medium are lower than those obtained when water or dilute nitric acid is the absorbing medium. Tests have been made with catalysts in the absorbing medium in an attempt to increase the rate of the controlling chemical reactions; however, no effective catalysts for this purpose have been reported (1).

The type of equipment used for the removal operation determines the magnitude of the contact area between the gas and the absorbing liquid. Experimental tests have shown that the rate of removal of nitrogen oxides from gases with aqueous absorption media is independent of the bulk liquid volume or bulk gas volume and is directly proportional to the interfacial area between the gas and the liquid (2). The controlling chemical reactions, therefore, must take place in the region

of contact between the gas and liquid phases.

#### Equipment for Removal of Nitrogen Oxides from Waste Gases

The preceding discussion indicates that two factors are of major importance in the development of improved methods for removing nitrogen oxides from waste gases: (1) Since the rates of the chemical reactions may control the rate of nitrogen oxides removal, a reasonably long time of contact between gas and liquid should be maintained, and (2) it is desirable to supply the maximum amount of gas-liquid contact area.

The chemical reactions involved in the removal process produce NO, and the absorption equipment must provide sufficient space for the occurrence of the slow oxidation of NO. However, this paper is concerned primarily with methods for obtaining the maximum removal efficiency for each gas-liquid contacting stage, and it is assumed that sufficient free space can be provided for the NO oxidation.

A variety of types of equipment can be used for the contacting operation. Bubble-cap towers, spray towers, packed towers, fritted bubblers, and Venturi atomizers are used for absorption operations. Removal of nitrogen oxides from gases can also be effected by adsorption on silica gel.

Although Venturi atomizers give a large interfacial area between the dispersed liquid droplets and the gas, this type of absorption unit is not effective for removing nitrogen oxides from gases because of the short contact time (1). Fritted bubblers permit a relatively long contact time and also give a large amount of contact area between the dispersed gas and the liquid. Therefore, despite the disadvantage of the high pressure drop involved in the operation of a fritted bubbler, this type of absorption unit could be useful for removing nitrogen oxides from dilute gases.

#### Experimental Results with Various types of Removal Equipment

Experimental data were obtained with a fritted bubbler, a packed tower, a spray tower, and a bubble-cap tower at gaseous concentration of  $e\text{NO}_2$  ranging from 0.2 to 2.0 per cent by volume. The essential information on the characteristics of the experimental equipment is presented in Table 1.

Water was fed to the units at a constant rate, and the flow rate was measured by a calibrated rotameter and checked by volumetric measurements. Gaseous nitrogen dioxide, obtained from cylinders containing  $\text{NO}_2$  and  $\text{N}_2\text{O}_4$ , was diluted with air and admitted at a steady rate to the lower section of the towers. The gas flow rates were measured by calibrated Venturi meters.

The towers were operated under steady conditions until equilibrium was attained as indicated by a constant acid concentration in the liquid product. Temperatures, pressures, and flow rates were read, and samples of the inlet gas, inlet liquid, and product liquid were taken. The liquid samples were analyzed by titrating a known volume with standard NaOH solution. The gas samples were taken in

evacuated bulbs containing hydrogen peroxide. The amount of gas sample was determined by weighing, and the amount of nitrogen oxides present was determined by titrating the nitric acid formed from the reaction between  $\text{H}_2\text{O}_2$  and  $\text{NO}_2$  and  $\text{N}_2\text{O}_4$ . From a knowledge of the flow rates and concentrations, it was possible to calculate the removal efficiency, expressed as the per cent of entering oxides removed.

The variables, such as gas rate, tower height, and liquid rate were chosen of magnitudes which would permit a fair comparison among the removal efficiencies of the various types of equipment. The values chosen represent as closely as possible those which would be used in corresponding industrial units.

The removal efficiency was found to be independent of the liquid rate in the bubble-cap tower and the fritted bubbler as long as the concentration of the liquid did not increase above 10 per cent by weight nitric acid. The spray tower was operated at a liquid rate which would give a finely dispersed mist, while the packed tower was operated at approximately 90 per cent of the liquid flooding velocity. A slot gas velocity of 1.17 ft/sec was used in the bubble-cap tower, while the gas rate used in the fritted bubbler was the rate at which well dispersed bubbles first appeared. Superficial gas velocities of 1.84 ft/sec were used in both the packed and spray towers.

Air was used as the diluent gas for all the test runs. The gas-liquid contact time in the bubble-cap and fritted-bubbler units was not sufficient for any appreciable oxidation of the NO formed in the chemical reactions. Some of the NO formed was oxidized to  $\text{NO}_2$  in the packed and spray towers; however, this difference in the operation is necessary in order to make a fair comparison among the various types of equipment.

Comparative results are presented in Figure 3 showing the effect of entering oxide concentration on the removal efficiencies for the different types of equipment. A reduction in oxide concentration causes a decrease in removal efficiency for all the types of equipment. Thus, as the gases become more dilute, the removal problem becomes more difficult.

The results obtained with the single-nozzle spray tower indicate very poor removal efficiencies at gaseous oxide concentrations less than about 1 per cent. At higher concentrations, the spray-tower efficiencies are comparable to those obtained in the other types of equipment. The use of multiple spray nozzles would, of course, cause a definite increase in the removal efficiency.

The removal efficiencies with the packed tower are lower than those found with the bubble-cap tower or fritted bubbler. It should be noted, however, that the decrease in efficiency with reduction in oxide content is fairly gradual, and, at nitrogen oxide concentrations less than about 0.2 per cent, the packed tower would be nearly as efficient as the other types of equipment.

From Figure 3, it can be seen that the fritted bubbler gives much better removal efficiencies than the other types of equipment tested. The pressure drop per stage for the fritted bubbler was approximately 30 times greater than the equivalent pressure drop for the



bubble-cap tower. Unless the gases were already under pressure, it would be expensive to add the equipment necessary to force a gas through a number of fritted-bubbler stages.

Since the removal efficiency of the bubble-cap tower approaches that of the fritted bubbler at low gaseous oxide concentrations, the optimum type of absorption equipment should combine the good features of both operations. A bubble-cap unit designed with a number of small gas outlets in the caps should approximate the beneficial effects of the small bubbles and large gas-liquid contact area found in a fritted bubbler.

The results shown in Figure 3 indicate that the silica gel adsorber gives the best removal efficiency of the units tested at gaseous concentrations less than 0.4 per cent nitrogen oxides. If essentially complete removal of the oxides is necessary, the silica gel adsorber should be used since the removal efficiency does not fall off rapidly at low gaseous concentrations.

#### NOMENCLATURE

- $A$  = gas-liquid interfacial area, sq cm.  
 $B$  = a constant at any temperature.  
 $DN_{2O_4}$  = gaseous diffusivity of  $N_2O_4$ , sq cm/sec.  
 $eNO_2$  =  $NO_2 + 2 N_2O_4$ .  
 $\ln F = (A/V_g) (DN_{2O_4}/x_F) 1.43 t$ .  
 $K_p$  = equilibrium constant for the reaction  $2 NO_2 = N_2O_4$ , atm<sup>-1</sup>.  
 $P_{fN_2O_4}$  = final partial pressure of  $N_2O_4$ , atm.  
 $P_{oN_2O_4}$  = original partial pressure of  $N_2O_4$ , atm.  
 $t$  = contact time, sec.  
 $V_g$  = volume of bulk of gas, cc.  
 $x_F$  = effective film thickness, cm.

#### REFERENCES

1. Andersen, L. B., and Johnstone, H. F., A.I.Ch.E. Journal, 1, 136 (1955).
2. Caudle, P. G., and Denbigh, K. G., Trans. Far. Soc., 49, 39 (1953).
3. Foster, E. G., and Daniels, F., Ind. Eng. Chem., 43, 986 (1951).
4. Klein, J. E., M. S. Thesis in Chem. Eng., Univ. of Ill. (1954).
5. Peters, M. S., Ross, C. P., and Klein, J. E., A.I.Ch.E. Journal, 1, 105 (1955).
6. Smith, J. H., and Daniels, F., J. Am. Chem. Soc., 69, 1735 (1947).
7. Verhoek, F. H., and Daniels, F., J. Am. Chem. Soc., 53, 1250 (1931).
8. Wenner, R. R., "Thermochemical Calculations," McGraw-Hill Book Co., Inc. (1941).

TABLE 1

TEST CONDITIONS USED FOR DETERMINING THE EFFICIENCY OF NITROGEN DIOXIDE  
REMOVAL FROM DILUTE GASES WITH DIFFERENT TYPES OF EQUIPMENT

Total pressure = 1 atmosphere  
Operating temperature = 25°C

Absorbent = Water. Gaseous diluent = Air

Type of Equipment	Gas Rate cu ft (S.C.) per min	Liquid Rate cc per min	Pressure Drop cm H <sub>2</sub> O	Remarks
Bubble-cap tower (one stage)	1.06 (slot velocity = 1.17 ft/sec)	300	1.8	Tower diameter = 7 1/2 in. Six bubble caps with 4 or 8 5/16-in. slots per cap. Liquid depth = 1 in. Distance between bubble-cap plate and top and bottom plates = 12 in.
Packed tower (1/4-in. glass Raschig rings)	0.53 (superficial vapor velocity = 1.84 ft/sec)	150	2.0 per foot of packed height	Tower diameter = 1 in. Packed height = 46 in. Efficiency expressed as per foot of packed height. No channeling observed.
Spray tower (1 No. T58- 1 mm spray nozzle)	0.53 (superficial vapor velocity = 1.84 ft/sec)	470	1.0	Tower diameter = 1 in. Tower height = 52 in. Finely dispersed spray directed countercurrent to rising gas. Negligible amount of liquid carryover in gas.
Fritted-glass bubbler (one stage)	0.53	300	59.0	Tower diameter = 5 1/2 in. 12 medium-frit glass rods. Fritted area = 1.03 sq in per rod. Liquid head over frits = 3 3/4 in.
Silica gel adsorber (No. 5 commercial gel - Ref. 1)	0.53 (superficial vapor velocity = 1.84 ft/sec)			Packed height = 12 in. Fraction saturated = 0.90. Time per cycle = 30 min. Efficiencies calculated from Ref. (2).

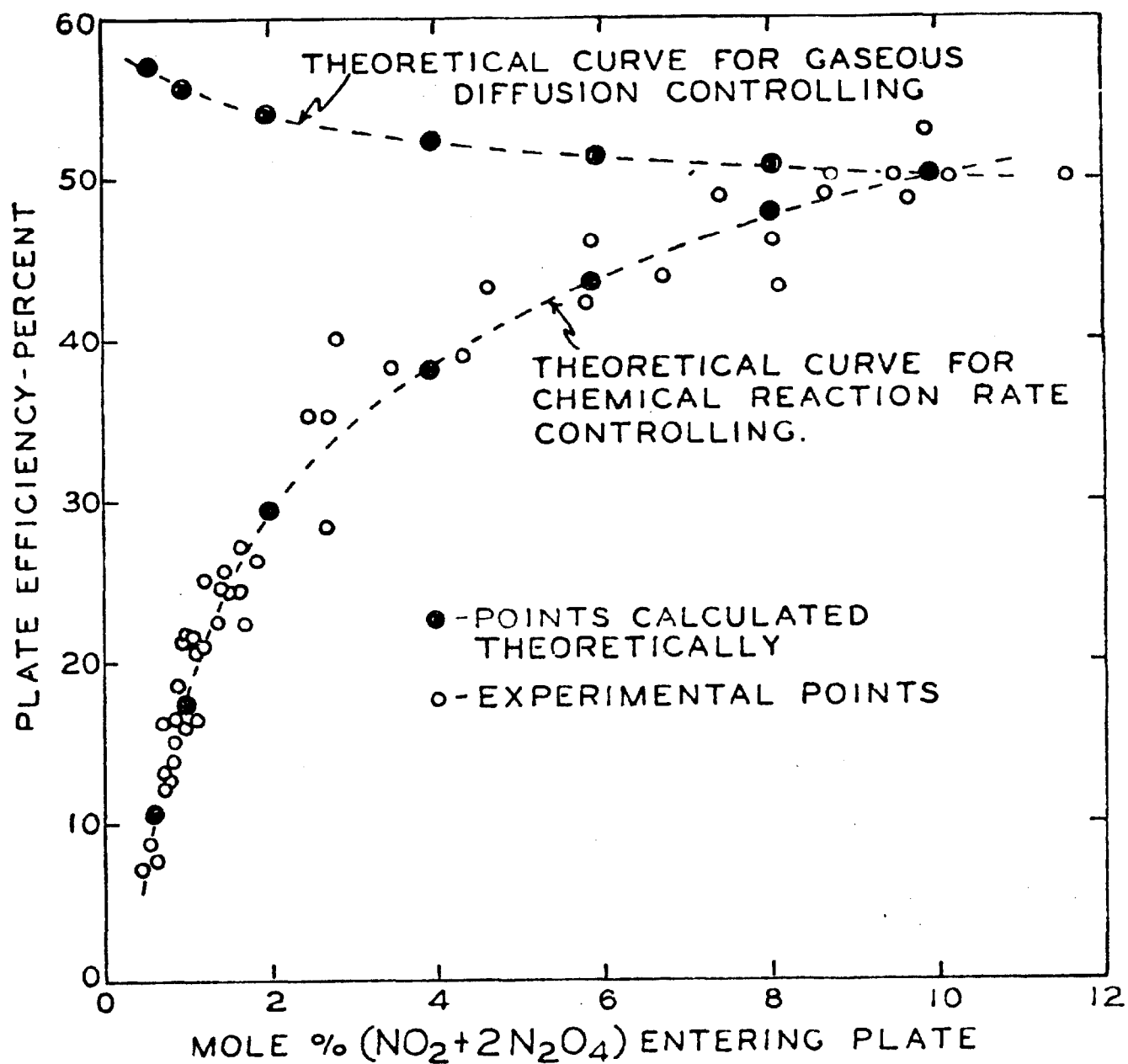


FIG. 1-EFFECT OF  $\text{NO}_2$  CONCENTRATION ON PLATE EFFICIENCY WITH ONE-PLATE BUBBLE-CAP TOWER (PRES.= 1 ATM., TEMP.= 23 °C., GAS SLOT VELOCITY = 1.18 FT./SEC.)

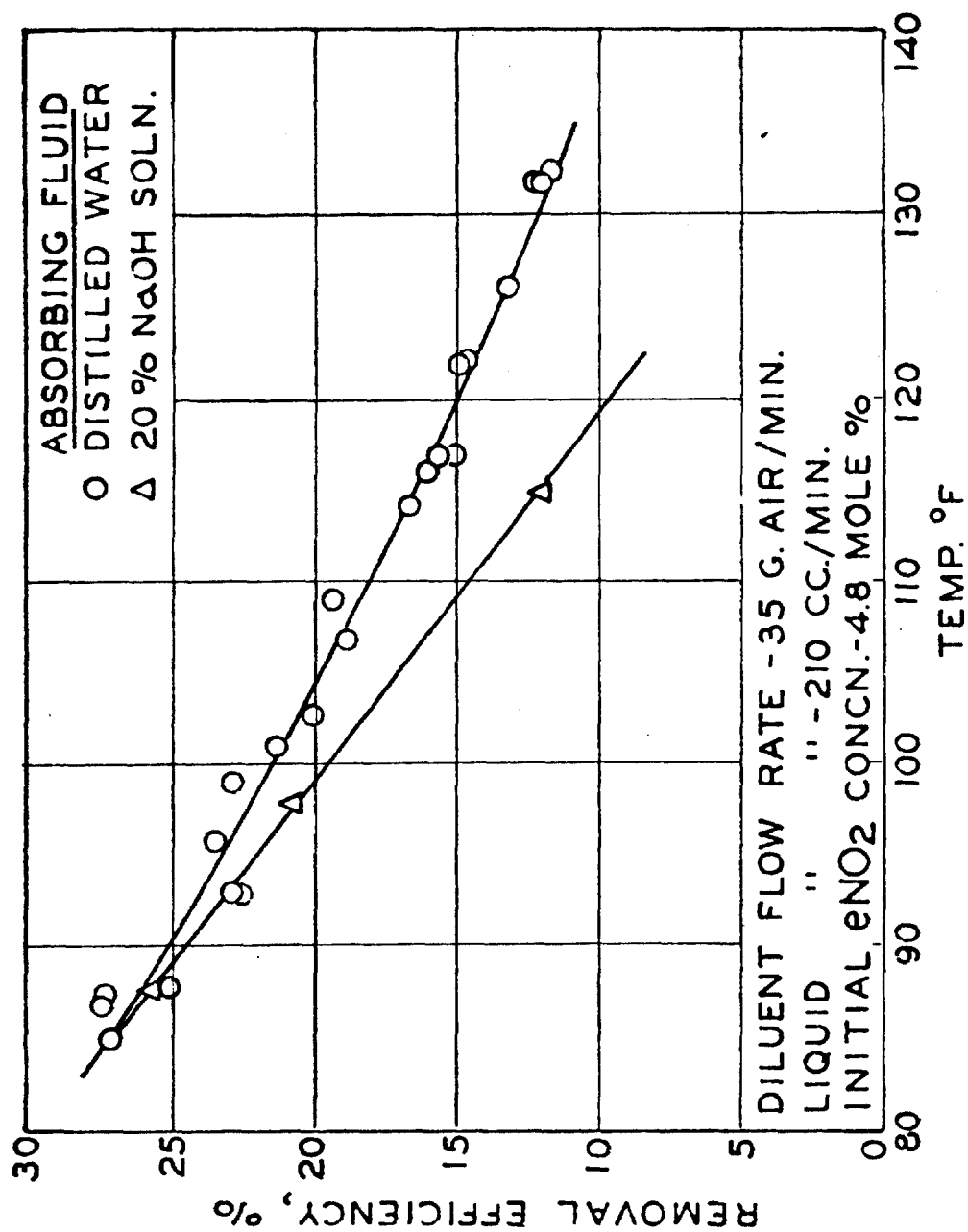


FIG. 2-EFFECT OF TEMPERATURE ON REMOVAL EFFICIENCY WITH WETTED-WALL TOWER (DIA.=2.15 CM.; HEIGHT=100 CM., PRES.=1 ATM.)

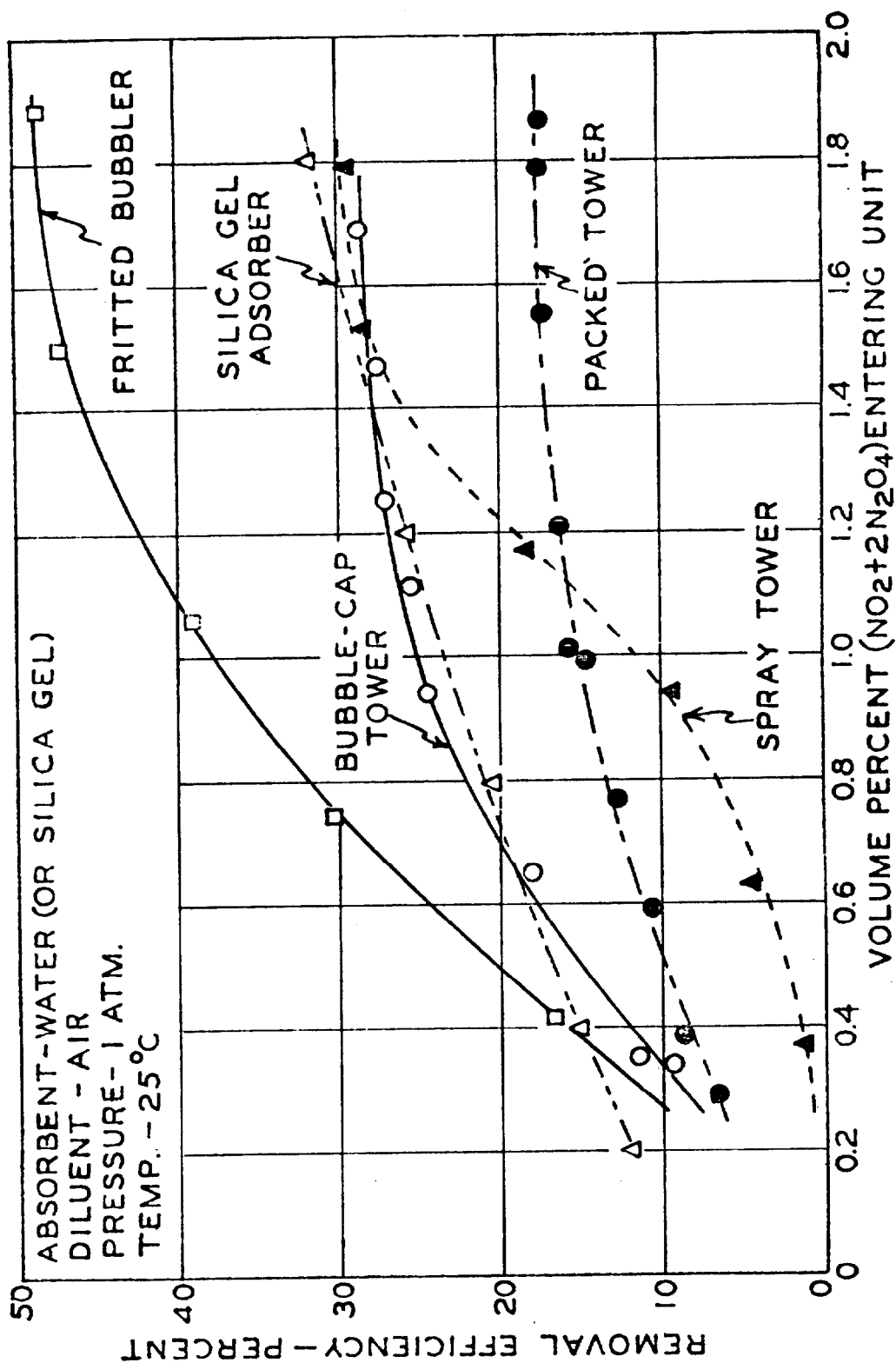


FIG. 3-EFFICIENCY OF NITROGEN DIOXIDE REMOVAL FROM DILUTE GASES WITH DIFFERENT TYPES OF EQUIPMENT